Propagation Behavior Of Partially Coherent General Model Vortex Higher-Order Cosh-Gaussian Beam In Biological Tissues

Halima Benzehoua[1], Faroq Saad[2], Abdelmajid Belafhal[1],
[1] Laboratory LPNAMME, Laser Physics Group, Department of Physics, Faculty of Sciences, Chouaïb Doukkali University, P. B 20, 24000 El Jadida, Morocco
[2] Department of Radiological Imaging Technologies, Cihan University-Erbil, Erbil, Kurdistan Region, Iraq

***Abstract*— Analytical expression for a partially coherent General Model vortex higher-order cosh-Gaussian beam (PCGMvHchGB) propagating in biological tissue medium is derived using extended Huygens-Fresnel method. Propagation characteristics of the PCGMvHchGB passing through biological tissue are discussed by some numerical results. The results indicate that the the PCGMvHchGB evolution is highly dependent on source beam parameters, including the spatial correlation length, decentered cosh and hollowness parameters, wavelength and orders of beam. Notably, the PCGMvHchGB in biological tissue transitions into a Gaussian beam more rapidly with smaller source parameters and further increasing propagation distance. This observation suggests that the resistance of PCGMvHchGB against turbulence is augmented with larger beam parameters. The significance of our findings lies in their potential applications in imaging technologies and bio-optical disease diagnosis.**

***Index Terms*— Extended Huygens-Fresnel method; Partially coherent General Model vortex higher-order cosh-Gaussian beam; Biological tissue.**

I. Introduction

In recent years, there has been a growing fascination with exploring the propagation properties of light beams in various optical mediums. This heightened interest stems from the extensive applications of laser technology in information encoding, optical communication and lattice spectroscopy [1-7]. Numerous scientists, including our research group members, which have conducted comprehensive works in this domain [8-16]. The evolution of technological imaging in medium of biological tissue using optical coherence tomography (OCT) method for disease diagnostics [17, 18], has brought to study the beam propagation in tissue mediums in detail [19-28] to the forefront of scientific inquiry. Biological tissue, a complex system characterized by strong light scattering due to spatial fluctuations in its refractive index, has become a subject of paramount importance. Schmitt and Kumar [29] investigated the statistical characteristics of refractive-index in medium of biological tissue, revealing spatial correlations akin to those induced in turbulent atmosphere.

On the other hand, the biological environment is recognized for its diverse the components of tissue which pose challenges to the transmission of optical signals. Many studies have shown that certain laser beams exhibit a reduced susceptibility to deterioration caused by turbulence. Vortex beams represent a specific category demonstrating such characteristics. Extensive research has been conducted the properties of various light beams, including stochastic electromagnetic vortex beams [19], anomalous hollow Gaussian beams [20], and both distributions of hollow Gaussian profiles[21], through turbulent biological tissues. Notably, Ebrahim and Belafhal have recently been presently partially Laguerre-Gaussian beams [22]. Furthermore, tow further works have been focused on the evolution study of hollow higher-order cosh-Gaussian beam and Generalized Hermite cosh-Gaussian beam in tissue medium named human upper dermis [29, 30].

Introducing a novel beam model, the GMvHchGB, Ebrahim et al. [31] presented a distinctive addition to the scientific discourse. Unlike the standard Gaussian beam, the GMvHchGB features two crucial parameters: the topological charge *l* and the decentered cosh. The vortex charge associated orbital angular momentum with the beam induces spiraling wave fronts. By selecting specific values for the decentered parameter and *l*, the GMvHchGB can be simplified to their special beams. Investigation of the characteristics of the GMvHchGB in a atmospheric turbulence revealed intriguing transformations, particularly in high turbulence conditions. Furthermore, the study extended to maritime turbulence, as explored by Chib et al. [32], and the impact on spectral intensity in the presence of human upper dermis tissue, as examined by Benzehoua et al. [33, 34]. Remarkably, there has been a notable absence of prior investigations into the behavior of PCGMvHchGB when traversing turbulent biological tissues. Hence, this paper aims to fill this research gap by studying the properties of PCGMvHchGB in biological tissues. The remainder of the paper is organized as follows. The theoretical model of PCGMvHchGB in turbulent biological tissues is calculated in Section 2. The beam evolutions in turbulent biological tissues are performed in Section 3. Finally, we conclude our results in Section 4.

To insert images in *Word,* position the cursor at the insertion point and either use Insert | Picture | From File or copy the image to the Windows clipboard and then Edit | Paste Special | Picture (with "float over text" unchecked).

Follow the instructions in this template before submitting your

DOI: http://doi.org/10.24086/biohs2024/paper.1302

camera-ready paper. Go to website for more information.

II. Propagation of PCGMvHchGB Through The Turbulent Biological Tissues

The cross-spectral density function of a PCGMvHchGB in the source plane (z=0) can be written as

$$W(\vec{r}_{01},\vec{r}_{02},z=0)=E(\vec{r}_{01},0)E^{*}(\vec{r}_{02},0)g(\vec{r}_{01}-\vec{r}_{02},z=0), \quad (1)$$

where the asterisk symbol * refer to the complex conjugation, $E(r_{0i},z=0)$ ($i=1$ *or* 2) indicates the electric field associated with a fully coherent GMvHchGB [31], which is given as

$$E(\vec{r}_{0i},z=0)=(x_0+i\,y_0)^{l}\cosh^{N}(\Omega x_0)\cosh^{N}(\Omega y_0)\exp\left(-\frac{x_0^2+y_0^2}{w_0^2}\right) \quad (2)$$

where $\vec{r}_{0i}=(x_{0i},y_{0i})$ is the position vector at the source plane, with (x_0, y_0) are the transverse coordinates, A_0 refers to the amplitude of the input field, l being the topological charge of the beam, N is the beam order, Ω is the parameter of the decentered cosh part, w_0 is the Gaussian waist radius.

$g(\vec{r}_{01}-\vec{r}_{02},z=0)$ indicates the degree of coherence of a Schell model source

$$g(\vec{r}_{01}-\vec{r}_{02},z=0)=\exp\left(-\frac{(\vec{r}_{01}-\vec{r}_{02})^2}{2\sigma_0^2}\right), \quad (3)$$

where σ_0 is the length of the spatial coherence at the input plane. By using the series transformation and Euler expansion [31], the input field in Eq. (1), can be re-written as

$$\begin{aligned}W(r_{01},r_{02},z=0)=&\frac{A_0}{2^{4N}}(x_{01}+iy_{01})^{l}(x_{02}+iy_{02})^{l}\sum_{m=0}^{N}\sum_{n=0}^{N}\binom{N}{m}\binom{N}{n}\sum_{m'=0}^{N}\sum_{n'=0}^{N}\binom{N}{m'}\binom{N}{n'}\exp\left(a_m^2+a_n^2\right)\exp\left(a_{m'}^2+a_{n'}^2\right)\\&\times\exp\left[-\left(\frac{x_{01}}{w_0}-a_m\right)^2\right]\exp\left[-\left(\frac{y_{01}}{w_0}-a_n\right)^2\right]\exp\left[-\left(\frac{x_{02}}{w_0}-a_{m'}\right)^2\right]\times\exp\left[-\left(\frac{y_{02}}{w_0}-a_{n'}\right)^2\right]\\&\times\exp\left[-\frac{(x_{01}-x_{01})^2}{2\sigma_0^2}\right]\exp\left[-\frac{(x_{02}-x_{02})^2}{2\sigma_0^2}\right],\end{aligned} \quad (4)$$

where $a_m=\left(m-\frac{N}{2}\right)\sqrt{\delta}$, and $a_n=\left(n-\frac{N}{2}\right)\sqrt{\delta}$, with $\delta=\Omega^2w_0^2$.

Let us now consider a biological tissue illuminated by laser beam. The physical model is given in Fig. 1.

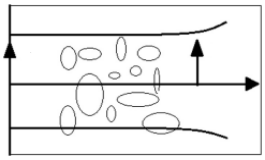

Figure 1: Schematic representation for a partially coherent beam in a biological tissue medium.

Based on the extended Huygens–Fresnel principle, the average intensity of a PCGMvHchGB traveling in a turbulent biological tissues at the plane z can be expressed as [36]

$$\begin{aligned}\langle I(\vec{r},z)\rangle=&\left(\frac{k}{2\pi z}\right)^2\int_{-\infty}^{+\infty}\int_{-\infty}^{+\infty}\int_{-\infty}^{+\infty}\int_{-\infty}^{+\infty}W(\vec{r}_{01},\vec{r}_{02},z=0)\\&\times\exp\left[-\frac{ik}{2z}\left\{(x_{01}-x)^2+(y_{01}-y)^2-(x_{02}-x)^2-(y_{02}-y)^2\right\}\right]\\&\times\left\langle\exp\left[\psi(\vec{r}_{01},\vec{r})+\psi^{*}(\vec{r}_{02},\vec{r})\right]\right\rangle d\vec{r}_{01}d\vec{r}_{02},\end{aligned} \quad (5$$

where $\vec{r}=(x,y)$ denotes the position vector at the received plane. $\psi(\vec{r}_{0i},\vec{r})$ indicates the random part related to a spherical wave at both source and output planes. $k=\frac{2\pi}{\lambda}$ refers to wavenumber of the beam with wavelength λ. $\langle\ \rangle$ and * indicates the ensemble average and the complex conjugate, and $d\vec{r}_{0i}=dx_{0i}dy_{0i}$ represents an elementary area at input plane.

Based on theory of Rytov, the term of an ensemble average is described as [36]

$$\left\langle\exp\left[\psi(\vec{r}_{01},\vec{r})+\psi^{*}(\vec{r}_{02},\vec{r})\right]\right\rangle=\exp\left[-\frac{1}{\rho_0^2}(\vec{r}_{01}-\vec{r}_{02})^2\right], \quad (6)$$

where the coherence length of a spherical wave in medium of turbulent tissue is given by $|\rho_0|=0.22\left(C_n^2k^2z\right)^{-1/2}$ with $C_n^2=\frac{\langle\delta n^2\rangle}{L_0^{2}(2-d_f)}$.

where the C_n^2 being a constant parameter in tissue medium named a refractive index structure. with $\langle\delta n^2\rangle$ is the ensemble represent the refractive index variance, L_0 means the outer scale of the size of refractive index and d_f is the tissue dimension fractal.

By using the following identities [35,37]

$$(x_0+i\,y_0)^{l}=\sum_{s=0}^{l}\binom{l}{s}x_0^{s}(iy_0)^{l-s} \quad (7)$$

$$\int_{-\infty}^{+\infty}x^{n}e^{-px^2+2qx}dx=\sqrt{\frac{\pi}{p}}\exp\left(\frac{q^2}{p}\right)\left(\frac{1}{2i\sqrt{p}}\right)^{n}H_n\left(\frac{iq}{\sqrt{p}}\right) \quad (8)$$

$$\int_{-\infty}^{+\infty}x^{l}H_m(\alpha x)e^{-px^2+2qx}dx=\frac{1}{2^{l}}\sqrt{\frac{\pi}{p}}\exp\left(\frac{q^2}{p}\right)\sum_{k=0}^{[m/2]}\frac{(-1)^k m!}{k!(m-2k)!}\left(\frac{\alpha}{i\sqrt{p}}\right)^{m+l-2k}H_{m+l-2k}\left(\frac{iq}{\sqrt{p}}\right) \quad (9)$$

with $\mathrm{Re}(p)>0$,

$$H_n(x+y)=\frac{1}{2^{n/2}}\sum_{k=0}^{n}\binom{n}{k}H_k\left(\sqrt{2}x\right)H_{n-k}\left(\sqrt{2}y\right), \quad (10)$$

and

$$H_n(x)=\sum_{k=0}^{[n/2]}\frac{(-1)^k n!}{k!(n-2k)!}(2x)^{n-2k} \quad (11)$$

where $H_n(x)$ indicates the Hermite polynomial of n order,

Substituting Eqs. (4) and (6) into Eq. (5), the result formula of received intensity distribution for a PCGMvHchGB in turbulent biological tissues as follows

$$\begin{aligned}\langle I(x,y,z)\rangle=&\frac{k^2}{4z^2}\frac{1}{2^{4N+3l/2}}\frac{1}{\sqrt{\alpha_{1,x}\alpha_{2,x}\alpha_{1,y}\alpha_{2,y}}}\sum_{m=0}^{N}\sum_{n=0}^{N}\binom{N}{m}\binom{N}{n}\sum_{s=0}^{l}\binom{l}{s}\sum_{m'=0}^{N}\sum_{n'=0}^{N}\binom{N}{m'}\binom{N}{n'}\sum_{s'=0}^{l}\binom{l}{s'}\\&\times i^{2l-s-s'}\exp\left(\frac{\gamma_{1,x}^2}{\alpha_{1,x}}+\frac{\gamma_{2,x}^2}{\alpha_{2,x}}\right)\left(\frac{1}{2i\sqrt{\alpha_{1,x}}}\right)^{s}\sum_{h=0}^{s}\binom{s}{h}H_{s-h}\left(\frac{i\sqrt{2}\gamma_{1,x}}{\sqrt{\alpha_1}}\right)\\&\times\sum_{\mu=0}^{[h/2]}\frac{(-1)^{\mu}h!}{\mu!(h-2\mu)!}\left(\frac{\sqrt{2}}{\rho_0^2\sqrt{\alpha_{1,x}\alpha_{2,x}}}\right)^{h+s'-2\mu}H_{h+s'-2\mu}\left(\frac{i\gamma_{2,x}}{\sqrt{\alpha_{2,x}}}\right)\\&\times\exp\left(\frac{\gamma_{1,y}^2}{\alpha_{1,y}}+\frac{\gamma_{2,y}^2}{\alpha_{2,y}}\right)\left(\frac{1}{2i\sqrt{\alpha_{1,y}}}\right)^{l-s}\sum_{h'=0}^{l-s}\binom{l-s}{h'}H_{l-s-h'}\left(\frac{i\sqrt{2}\gamma_{1,y}}{\sqrt{\alpha_{1,y}}}\right)\\&\times\sum_{\mu'=0}^{[h'/2]}\frac{(-1)^{\mu'}h'!}{\mu'!(h'-2\mu')!}\left(\frac{\sqrt{2}}{\rho_0^2\sqrt{\alpha_{1,x}\alpha_{2,y}}}\right)^{h'+l-s'-2\mu'}H_{h'+l-s'-2\mu'}\left(\frac{i\gamma_{2,y}}{\sqrt{\alpha_{2,y}}}\right).\end{aligned} \quad (12)$$

The parameters presented in the last equation are defined as

DOI: http://doi.org/10.24086/biohs2024/paper.1302

$$\alpha_{1,x} = \alpha_{1,y} = \frac{1}{\omega_0^2} + \frac{ik}{2z} + \frac{1}{2\sigma^2} + \frac{1}{\rho_0^2}, \quad (13)$$

$$\gamma_{1,x} = \frac{a_m}{\omega_0} + \frac{ikx}{2z} \quad (14)$$

$$\gamma_{1,y} = \frac{a_n}{\omega_0} + \frac{iky}{2z} \quad (15)$$

$$\alpha_{2,x} = \frac{1}{\omega_0^2} + \frac{1}{\rho_0^2} - \frac{ik}{2z} - \frac{\eta^2}{\alpha_{1,x}} \quad (16)$$

$$\alpha_{2,y} = \frac{1}{\omega_0^2} + \frac{1}{\rho_0^2} - \frac{ik}{2z} - \frac{\eta^2}{\alpha_{1,y}} \quad (17)$$

$$\gamma_{2,x} = \frac{a_{m'}}{\omega_0} - \frac{ikx}{2z} + \frac{\gamma_{1,x}\eta}{\alpha_{1,x}} \quad (18)$$

$$\gamma_{2,y} = \frac{a_{n'}}{\omega_0} - \frac{iky}{2z} + \frac{\gamma_{1,y}\eta}{\alpha_{1,y}} \quad (19)$$

And

$$\eta = \frac{1}{2\sigma^2} + \frac{1}{\rho_0^2}. \quad (20)$$

In coming section, according to the above theoretical result, numerical examples are simulated to discuss the properties of PCGMvHchGB in both different mediums of biological tissues including mouse focusing on intestinal epithelium and deep dermis of mouse.

III. Numerical Results

Based on the analytical formula derived by Eq. (12), numerous numerical simulations conducted to elucidate the properties of the PCGMvHchGB in turbulent biological tissue, considering variations in the associated parameters. The parameters are chosen as: $\Omega = 0.4\mu m^{-1}$, $\lambda = 0.6328\,\mu m$, $w_0 = 2\mu m$, $C_n^2 = 0.22\times10^{-3}\,\mu m^{-1}$, $\sigma_0 = 3\,\mu m$, $z = 4\mu m$ l=1 and N=1.

Fig. 2 illustrates the varied configurations of the PCGMvHchGB in tow different tissues mediums for various beam orders. The consistent effect of N is observed in both mediums of tissues including deep dermis of mouse $C_n^2 = 0.22\times10^{-3}\,\mu m^{-1}$ and the human upper dermis $C_n^2 = 0.44\times10^{-3}\,\mu m^{-1}$ (Schmitt and Kumar, 1996). The average intensity exhibits a dark spot center of zero intensity, that becomes larger with increasing N. At z=6.5 µm, the distribution of the intensity of the PCGMvHchGB will change into a Gaussian profile. With further increases N (N=3), the PCGMvHchGB takes a flattened shape. A comparison between Fig. 2-A and Fig. 2-B reveals that the propagation behavior of the PCGMvHchGB within the deep dermis of mouse will evolve into a Gaussian beam. One can also observe that the PCGMvHchGB within biological tissues demonstrates enhanced resilience against turbulence when N is larger.

The average intensity of PCGMvHchGB in biological tissues for various topological charge l at several distances of propagation is presented in Fig. 3. The curves of this figure reveal that PCGMvHchGB keeps its original pattern for some distance of propagation. As the propagation distance increases, the beam profile changes gradually into a flat-topped shape and will take a Gaussian pattern at the far-field. The PCGMvHchGB evolution into a Gaussian profile can be demonstrated that, in the far field, the received intensity undergoes a transition into completely incoherent light because of the impact of the tissue medium [38].

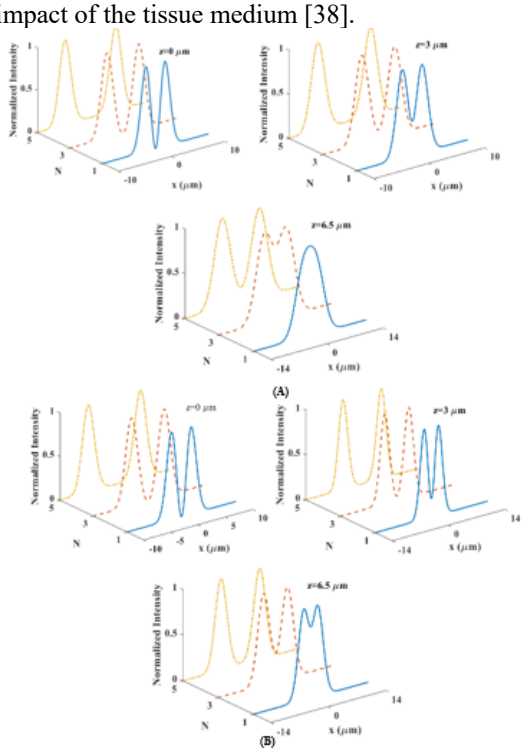

Figure 2: (Color online) Normalized intensity of PCGMvHchGB for two types of tissues and different beam orders N with **(A)** $C_n^2 = 0.22\times10^{-3}\,\mu m^{-1}$ and **(B)** $C_n^2 = 0.44\times10^{-3}\,\mu m^{-1}$.

It is evident that the topological charge l in the PCGMvHchGB model plays a critical role in influencing performance in conditions of biological tissue medium. Results suggest that a larger l imparts a higher ability to resistance the tissues conditions.

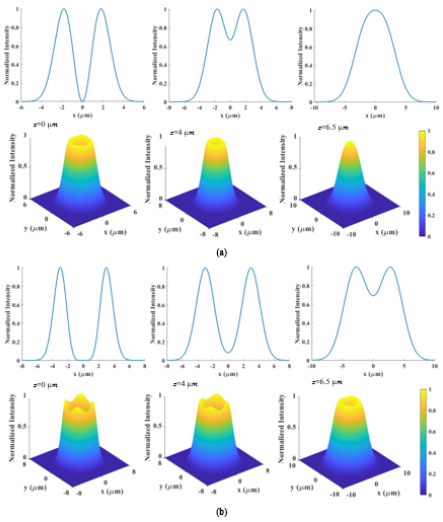

Figure 3: The normalized intensity of PCGMvHchGB during its propagation in turbulent biological tissue for various values of propagation distances with **(a)** $l = 1$ and **(b)** $l = 3$.

Fig. 4 demonstrates how the beam parameter influences the average intensity of PCGMvHchGB in tissue medium. The

DOI: http://doi.org/10.24086/biohs2024/paper.1302

similar behavior of the hollow beam profile shows when beam parameters are increased.

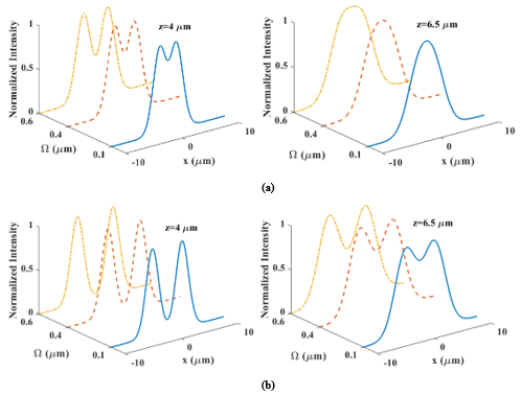

Figure 4: Evolution of the normalized intensity of PCGMvHchGB during its propagation in turbulent biological tissue for various values of Ω and at two propagation distances with **(a)** $l = 1$ and **(b)** $l = 3$.

One can also show from the plots that beam with smaller parameters, the Gaussian profile region becomes larger as increasing the distance of PCGMvHchGB propagation in turbulent biological tissue.

In Fig. 5, the normalized intensity of PCGMvHchGB is illustrated for some values of wavelengths at different distances. Based on the observations in Fig. 5, one can infer that with increasing distance in biological tissue, the average intensity undergoes a hollow spot pattern to a flat-topped profile, and culminating in a Gaussian distribution. Furthermore, it is noteworthy that the distribution of beam evolution with a larger propagation distance and a smaller wavelength can be observed to occur more rapidly.

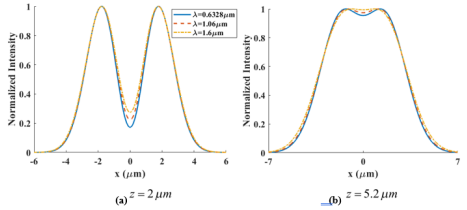

Figure 5: Normalized intensity of PCGMvHchGB for various wavelengths and two propagation distances.

To demonstrate the spatial correlation length effect on the PCGMvHchGB in biological tissue medium, numerical discussions are presented in Fig. 6 at various spatial correlation length: (a) $\sigma_0 = 0.55\,\mu m$ and (b) $\sigma_0 = 3\,\mu m$. As depicted in Fig. 6(a)-(b), Based on conditions of beam parameters at different distances z, the distribution of intensity pattern of the PCGMvHchGB undergoes transforms throughout the propagation, regardless of the length of spatial correlation. It is observed that the beam initially possesses a central dark hollow pattern that diminishes during their propagation through turbulent biological tissue, transforming into a Gaussian profile, accompanied by a decrease in the maximum peak intensity. It is noteworthy that the beam with smaller spatial correlation length, diffracted beam pattern undergoes rapid changes, i.e., over a shorter distance of propagation.

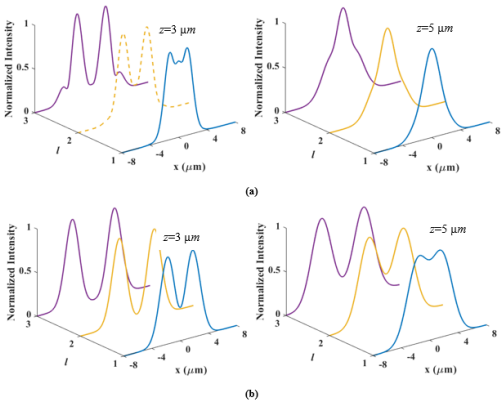

Figure 6: Normalized intensity of PCGMvHchGB for two propagation distances and (a) $\sigma_0 = 0.55\,\mu m$ and (b) $\sigma_0 = 3\mu m$.

Conclusion

We have presented the properties of PCGMvHchGB through turbulent biological tissue, specifically the upper dermis of human. Utilizing the Huygens-Fresnel diffraction integral, we derive the field expression and investigate the distribution of intensity for the PCGMvHchGB through numerical examples. The analysis considers the influence of both turbulent conditions in the biological tissue and various source beam parameters, such as the spatial correlation length, hollowness and decentered cosh parameters, wavelength and orders of beam. The obtained results underscore the sensitivity of the received intensity distribution to the source beam parameters. Notably, when the increase distance, the PCGMvHchGB with parameters are smaller in the biological tissue transitions into a Gaussian beam more rapidly. This observation implies an increased resistance of the PCGMvHchGB against turbulence with a higher source parameter..

References

[1] Yadav, B.K., Bisht, N.S., Mehrotra, R., Kandpal, H.C.: Diffraction-induced spectral anomalies for information encoding and information hiding – Possibilities and limitations. Opt. Commun. 277, 24–32 (2007).

[2] Yadav, B.K., Rizvi, S.A.M., Raman, S., Mehrotra, R., Kandpal, H.C.: Information encoding by spectral anomalies of spatially coherent light diffracted by an annular aperture. Opt. Commun. 269, 253–260 (2007).

[3] Yadav, B.K., Raman, S., Kandpal, H.C.: Information exchange in free spacing using spectral switching of diffracted polychromatic light: possibilities and limitations. J. Opt. Soc. Am. A 25, 2952–2959 (2008).

[4] Benzehoua, H., Saad, F., Belafhal, A.: A theoretical study of spectral properties of generalized chirped Hermite cosh Gaussian pulse beams in oceanic turbulence. Opt. Quant. Electron. 55, 1-14 (2023).

[5] Saad, F.: Propagation properties of general model vortex higher-order Cosh-Gaussian laser beam through uniaxial crystal orthogonal to the optical axis. Opt. Quant. Electron. 56, 790 (1-15) (2024).

[6] Saad, F., Benzehoua, H., Belafhal, A.: Evolution properties of Laguerre higher order cosh Gaussian beam propagating through fractional Fourier transform optical system. Opt. Quant. Electron. 56, 1-15 (2024).

DOI: http://doi.org/10.24086/biohs2024/paper.1302

[7] Saad, F., Hricha, Z., Belafhal, A.: Propagation properties of higher-order cosine-hyperbolic-Gaussian beams in a chiral medium. Opt. Quant. Electron. 56, 1-15 (2024).

[8] Zhong, Y., Cui, Z., Shi, J., Qu, J.: Propagation properties of partially coherent Laguerre–Gaussian beams in turbulent atmosphere. Opt. Laser Technol. 43, 741-747 (2011).

[9] Benzehoua, H., Belafhal, A.: Analysis of the behavior of pulsed vortex beams in oceanic

turbulence. Opt. Quant. Electron. 55, 1-14 (2023).

[10] Benzehoua, H., Belafhal, A.: Analyzing the spectral characteristics of a pulsed Laguerre higher-order cosh-Gaussian beam propagating through a paraxial ABCD optical system. Opt. Quant. Electron. 55, 663-681 (2023).

[11] Benzehoua, H., Belafhal, A.: Effects of Hollow–Gaussian beams on Fresnel diffraction by an opaque disk. Quant. Electron. 55, 1-16 (2023).

[12] Benzehoua, H., Belafhal, A.: The Effects of Atmospheric Turbulence on the Spectral Changes of Diffracted Pulsed Hollow Higher-Order Cosh-Gausian Beam. Opt. Quant. Electron. 55, 973-993 (2023).

[13] Benzehoua, H., Belafhal, A.: Spectral properties of pulsed Laguerre higher-order cosh-Gaussian beam propagating through the turbulent atmosphere. Opt. Commun. 541, 129492-129502 (2023).

[14] Benzehoua, H., Bayraktar, M., Belafhal, A.: Influence of maritime turbulence on the spectral changes of pulsed Laguerre higher-order cosh-Gaussian beam. Opt. Quant. Electron. 56, 155-169 (2023).

[15] Saad, F., Benzehoua, H., Belafhal, A.: Propagation behavior of a generalized Hermite cosh-Gaussian laser beam through marine environment. Opt. Quant. Electron. 56, 1-12 (2023).

[16] Saad, F., Benzehoua, H., Belafhal, A.: Oceanic turbulent effect on the received intensity of a generalized Hermite cosh-Gaussian beam. Opt. Quant. Electron. 56, 1-15 (2023).

[17] D. Huang, E. A. Swanson, C. P. Lin, J. S. Schuman, W. G. Stinson, W. Chang, M. R. Hee, T. Flotte, K. Gregory, C. A. Puliafito, Optical coherence tomography, Science 254, 1178-1181 (1991).

[18] G. Husler, M. W. Lindner, Coherence radar and spectral radarnew tools for dermatological diagnosis, J. Biomed. Opt. 3, 21-31 (1998).

[19] Luo, M., Chen, Q., Hua, L., Zhao, D.: Propagation of stochastic electromagnetic vortex

beams through the turbulent biological tissues. Phys. Lett. A 378, 308-314 (2014).

[20] Lu, X., Zhu, X., Wang, K., Zhao, C., Cai, Y.: Effects of biological tissues on the propagation properties of anomalous hollow beams. Optik 127, 1842-1847 (2016).

[21] Saad, F., Belafhal, A.: A theoretical investigation on the propagation properties of Hollow Gaussian beams passing through turbulent biological tissues. Optik 141, 72-82 (2017).

[22] Ebrahim, A. A. A., Belafhal, A.: Effect of the turbulent biological tissues on the propagation properties of Coherent Laguerre-Gaussian beams. Opt. Quant. Electron. 53, 179-196 (2021).

[23] Chib, S., Dalil-Essakali, L., Belafhal A.: Partially coherent beam propagation in turbid tissue-like scattering medium. Opt. Quant. Electron. 55, 602-617 (2023).

[24] Duan, M., Tian, Y., Zhang, Y., Li, J.: Influence of biological tissue and spatial correlation on spectral changes of Gaussian-Schell model vortex beam. Optics and Lasers in Engineering, 134, 106224-106230 (2020).

[25] Cheng, K., Zhu, B. Y., Shu, L.Y., Liao, S., Liang, M.T.: Averaged intensity and spectral shift of partially coherent chirped optical coherence vortex lattices in biological tissue turbulence, J. Chinese Optics 15, 364-372 (2022).

[26] Benzehoua, H., Saad, F., Belafhal, A.: Spectrum changes of pulsed chirped Generalized Hermite cosh-Gaussian beam through turbulent biological tissues. Optik 294, 171440-171451 (2023).

[27] Bayraktar M.: Propagation of partially coherent hyperbolic sinusoidal Gaussian beam in biological tissue. Optik. 245, 167741-167749 (2021).

[28] Schmitt JM, Kumar G, Turbulent nature of refractive-index variations in biological tissue. Opt Lett 21, 1310–1312 (1996).

[29] Bayraktar, M., Elmabruk, K., Duncan, J. C. M., Chatzinotas, S.: Propagation of hollow higher order cosh-Gaussian beam in human upper dermis. Phys. Scr. 98, 115538-115548 (2023).

[30] Saad, F., Benzehoua, H., Belafhal, A.: Analysis on the propagation characteristics of a Generalized Hermite cosh-Gaussian beam through human upper dermis tissue. Opt. Quant. Electron. 56, 1-15 (2024).

[31] Ebrahim, A.A.A., Swillam, M. A., Belafhal, A.: Atmospheric turbulent effects on the propagation properties of a General Model vortex Higher-order cosh-Gaussian beam. Opt. Quant. Electron. 55, 1-13 (2023).

[32] Chib, S., Khannous, F., Belafhal, A.: Propagation of General Model vortex higher-order cosh-Gaussian beam in maritime turbulence. Opt. Quant. Electron. 55, 1-12 (2023).

[33] Benzehoua, H., Saad, F., Bayraktar, M., Chatzinotas, S., Belafhal, A. :Impact of human upper dermis tissue on the spectral intensity of a pulsed chirped general model vortex higher-order cosh-Gaussian beam. Opt. Quant. Electron. 56, 850 (1-16) (2024).

[34] Benzehoua, H., Saad, F., Bayraktar, M., Chatzinotas, S., Belafhal, A. : Analyzing the theoretical evolution behavior of Laguerre higher-order cosh-Gaussian beam propagating through liver tissue. Opt. Quant. Electron. 56, 767(1-14) (2024).

[35] Gradshteyn, I.S., Ryzhik, I.M.: Tables of Integrals, Series, and Products, fifth ed., Academic Press, New York, (1994).

[36] Andrews, L. C., Philips, R. L.: Laser beam propagation through Random media. SPIE Press, Washington (1998).

[37] Belafhal, A., Hricha, Z., Dalil-Essakali L., Usman, T.: A note on some integrals involving Hermite polynomials encountered in caustic optics. Adv. Math. Models App. 5, 313-319 (2020).

[38] Eyyuboglu, H. T. and Baykal, Y., Scintillation characteristics of cosh-Gaussian beams, App. Opt., 46, 1099-1106 (2007).

DOI: http://doi.org/10.24086/biohs2024/paper.1302